A Spectral Method for Elliptic Equations: The Neumann Problem

Kendall Atkinson
Departments of Mathematics & Computer Science
The University of Iowa

David Chien, Olaf Hansen
Department of Mathematics
California State University San Marcos

July 6, 2009

Abstract

Let Ω be an open, simply connected, and bounded region in $\mathbb{R}^d$, $d \geq 2$, and assume its boundary $\partial\Omega$ is smooth. Consider solving an elliptic partial differential equation $-\Delta u + \gamma u = f$ over Ω with a Neumann boundary condition. The problem is converted to an equivalent elliptic problem over the unit ball B, and then a spectral Galerkin method is used to create a convergent sequence of multivariate polynomials u_n of degree $\leq n$ that is convergent to u. The transformation from Ω to B requires a special analytical calculation for its implementation. With sufficiently smooth problem parameters, the method is shown to be rapidly convergent. For $u \in C^{\infty}\left(\overline{\Omega}\right)$ and assuming $\partial\Omega$ is a C^{∞} boundary, the convergence of $\|u - u_n\|_{H^1}$ to zero is faster than any power of $1/n$. Numerical examples in $\mathbb{R}^2$ and $\mathbb{R}^3$ show experimentally an exponential rate of convergence.

1 INTRODUCTION

Consider solving the Neumann problem for Poisson's equation:

$$-\Delta u + \gamma(s)u = f(s), \qquad s \in \Omega \tag{1}$$

$$\frac{\partial u(s)}{\partial n_s} = g(s), \qquad s \in \partial\Omega. \tag{2}$$

Assume Ω is an open, simply-connected, and bounded region in $\mathbb{R}^d$, $d \geq 2$, and assume that its boundary $\partial\Omega$ is several times continuously differentiable. Similarly, assume the functions $\gamma(s)$ and $f(s)$ are several times continuously differentiable over $\overline{\Omega}$, and assume that $g(s)$ is several times continuously differentiable over the boundary $\partial\Omega$.

There is a rich literature on spectral methods for solving partial differential equations. From the more recent literature, we cite [7], [8], [9], and [15]. Their bibliographies contain references to earlier papers on spectral methods. The present paper is a continuation of the work in [3] in which a spectral method is given for a general elliptic equation with a Dirichlet boundary condition. Our approach is somewhat different than the standard approaches. We convert the partial differential equation to an equivalent problem on the unit disk or unit ball, and in the process we are required to work with a more complicated equation. Our approach is reminiscent of the use of conformal mappings for planar problems. Conformal mappings can be used with our approach when working on planar problems, although having a conformal mapping is not necessary.

In §2 we assume that (1)-(2) is uniquely solvable, and we present a spectral Galerkin method for its solution. In §3 we extend the method to the problem with $\gamma(s) \equiv 0$ in Ω. The problem is no longer uniquely solvable and we extend our spectral method to this case. The implementation of the method is discussed in §4 and it is illustrated in §5.

2 A spectral method for the uniquely solvable case

We assume the Neumann problem (1)-(2) is uniquely solvable. This is true, for example, if

$$\gamma(s) \geq c_\gamma > 0, \qquad s \in \overline{\Omega} \tag{3}$$

for some constant $c_\gamma > 0$. For functions $u \in H^2(\Omega)$, $v \in H^1(\Omega)$,

$$\begin{aligned} \int_\Omega v(s)\left[-\Delta u(s) + \gamma(s)u\right] ds = \int_\Omega \left[\nabla u(s) \cdot \nabla v(s) + \gamma(s)u(s)v(s)\right] ds \\ - \int_{\partial\Omega} v(s) \frac{\partial u(s)}{\partial n_s} ds. \end{aligned} \tag{4}$$

Introduce the bilinear functional

$$\mathcal{A}(v_1, v_2) = \int_\Omega \left[\nabla v_1(s) \cdot \nabla v_2(s) + \gamma(s)v_1(s)v_2(s)\right] ds. \tag{5}$$

The variational form of the Neumann problem (1)-(2) is as follows: find u such that

$$\mathcal{A}(u, v) = \ell_1(v) + \ell_2(v), \qquad \forall v \in H^1(\Omega) \tag{6}$$

with the linear functionals defined by

$$\ell_1(v) = \int_\Omega v(s) f(s)\, ds, \tag{7}$$

$$\ell_2(v) = \int_{\partial\Omega} v(s)\, g(s)\, ds. \tag{8}$$

The norms we use for ℓ_1 and ℓ_2 are the standard operator norms when regarding ℓ_1 and ℓ_2 as linear functionals on $H^1(\Omega)$. The functional ℓ_1 is bounded easily on $H^1(\Omega)$,

$$|\ell_1(v)| \leq \|f\|_{L^2}\|v\|_{L^2} \leq \|f\|_{L^2}\|v\|_{H^1}. \tag{9}$$

Ordinarily, we will use $\|v\|_1$ in place of $\|v\|_{H^1}$.

The functional ℓ_2 is bounded (at least for bounded domains Ω). To show this, begin by noting that the restriction $\rho : H^1(\Omega) \to H^{1/2}(\partial\Omega)$ is continuous [13, Th. 3.37] and the imbedding $\iota : H^{1/2}(\partial\Omega) \hookrightarrow L^2(\partial\Omega)$ is compact [13, Th. 3.27]. If we further denote by l_g the continuous mapping

$$l_g : u \mapsto \int_{\partial\Omega} u(s)g(s)\,ds, \qquad u \in L^2(\partial\Omega)$$

then we see $\ell_2 = l_g \circ \iota \circ \rho$, and therefore ℓ_2 is bounded.

It is straightforward to show $\mathcal{A}$ is bounded,

$$\begin{gathered} |\mathcal{A}(v,w)| \leq c_{\mathcal{A}}\|v\|_1\|w\|_1, \\ c_{\mathcal{A}} = \max\{1, \|\gamma\|_\infty\}. \end{gathered} \tag{10}$$

In addition, we assume $\mathcal{A}$ is strongly elliptic on $H^1(\Omega)$,

$$\mathcal{A}(v,v) \geq c_e\|v\|_1^2, \qquad v \in H^1(\Omega) \tag{11}$$

with some $c_e > 0$. This follows ordinarily from showing the unique solvability of the Neumann problem (1)-(2). If (3) is satisfied, then we can satisfy (11) with

$$c_e = \min\{1, c_\gamma\}$$

Under our assumptions on $\mathcal{A}$, including the strong ellipticity in (11), the Lax-Milgram Theorem implies the existence of a unique solution u to (6) with

$$\|u\|_1 \leq \frac{1}{c_e}\left[\|\ell_1\| + \|\ell_2\|\right]. \tag{12}$$

Our spectral method is defined using polynomial approximations over the open unit ball in $\mathbb{R}^d$, call it B_d. Introduce a change of variables

$$\Phi : \overline{B}_d \underset{onto}{\overset{1-1}{\longrightarrow}} \overline{\Omega}$$

with Φ a twice-differentiable mapping, and let $\Psi = \Phi^{-1} : \overline{\Omega} \underset{onto}{\overset{1-1}{\longrightarrow}} \overline{B}_d$. [We comment later on the creation of Φ for cases in which only the boundary mapping $\phi : \partial B_d \to \partial\Omega$ is known.] For $v \in L^2(\Omega)$, let

$$\widetilde{v}(x) = v(\Phi(x)), \qquad x \in \overline{B}_d \subseteq \mathbb{R}^d$$

and conversely,

$$v(s) = \widetilde{v}(\Psi(s)), \qquad s \in \overline{\Omega} \subseteq \mathbb{R}^d.$$

Assuming $v \in H^1(\Omega)$, we can show

$$\nabla_x \widetilde{v}(x) = J(x)^{\mathrm{T}} \nabla_s v(s), \qquad s = \Phi(x)$$

with $J(x)$ the Jacobian matrix for Φ over the unit ball B_d,

$$J(x) \equiv (D\Phi)(x) = \left[\frac{\partial \Phi_i(x)}{\partial x_j}\right]_{i,j=1}^{d}, \qquad x \in \overline{B}_d.$$

Similarly,

$$\nabla_s v(s) = K(s)^{\mathrm{T}} \nabla_x \widetilde{v}(x), \qquad x = \Psi(s)$$

with $K(s)$ the Jacobian matrix for Ψ over Ω. Also,

$$K(\Phi(x)) = J(x)^{-1}. \tag{13}$$

Using the change of variables $s = \Phi(x)$, the formula (5) converts to

$$\begin{aligned}
\mathcal{A}(v_1, v_2) &= \int_{B_d} \{[K(\Phi(x))^{\mathrm{T}} \nabla_x \widetilde{v}_1(x)]^{\mathrm{T}} [K(\Phi(x))^{\mathrm{T}} \nabla_x \widetilde{v}_2(x)] \\
&\qquad + \gamma(\Phi(x)) v_1(\Phi(x)) v_2(\Phi(x)\} \, |\det[J(x)]| \, dx \\
&= \int_{B_d} \{[J(x)^{-\mathrm{T}} \nabla_x \widetilde{v}_1(x)]^{\mathrm{T}} [J(x)^{-\mathrm{T}} \nabla_x \widetilde{v}_2(x)] \\
&\qquad + \widetilde{\gamma}(x) \widetilde{v}_1(x) \widetilde{v}_2(x)\} \, |\det[J(x)]| \, dx \\
&= \int_{B_d} \{\nabla_x \widetilde{v}_1(x)^{\mathrm{T}} A(x) \nabla_x \widetilde{v}_2(x) + \widetilde{\gamma}(x) \widetilde{v}_1(x) \widetilde{v}_2(x)\} |\det[J(x)]| \, dx \\
&\equiv \widetilde{\mathcal{A}}(\widetilde{v}_1, \widetilde{v}_2)
\end{aligned} \tag{14}$$

with

$$A(x) = J(x)^{-1} J(x)^{-\mathrm{T}}.$$

We can also introduce analogues to ℓ_1 and ℓ_2 following a change of variables, calling them $\widetilde{\ell}_1$ and $\widetilde{\ell}_2$ and defined on $H^1(B_d)$. For example,

$$\widetilde{\ell}_1(\widetilde{v}) = \int_{B_d} \widetilde{v}(x) f(\Phi(x)) \, |\det[J(x)]| \, dx.$$

We can then convert (6) to an equivalent problem over $H^1(B_d)$. The variational problem becomes

$$\widetilde{\mathcal{A}}(\widetilde{u}, \widetilde{v}) = \widetilde{\ell}_1(\widetilde{v}) + \widetilde{\ell}_2(\widetilde{v}), \qquad \forall \widetilde{v} \in H^1(B_d). \tag{15}$$

The assumptions and results in (6)-(11) extend to this new problem on $H^1(B_d)$. The strong ellipticity condition (11) becomes

$$\begin{aligned}
\widetilde{\mathcal{A}}(\widetilde{v}, \widetilde{v}) &\geq \widetilde{c}_e \|\widetilde{v}\|_1^2, \qquad \widetilde{v} \in H^1(B_d), \\
\widetilde{c}_e &= c_e \frac{\min_{x \in \overline{B}_d} |\det J(x)|}{\max\left[1, \max_{x \in \overline{B}_d} \|J(x)\|_2^2\right]}
\end{aligned} \tag{16}$$

where $\|J(x)\|_2$ denotes the operator matrix 2-norm of $J(x)$ for $\mathbb{R}^d$. Also,

$$\left|\widetilde{\mathcal{A}}(\widetilde{v},\widetilde{w})\right| \leq \widetilde{c}_{\mathcal{A}} \|\widetilde{v}\|_1 \|\widetilde{w}\|_1,$$

$$\widetilde{c}_{\mathcal{A}} = \left\{\max_{x\in\overline{B}_d} |\det[J(x)]|\right\} \max\left\{\max_{x\in\overline{B}_d} \|A(x)\|_2, \|\gamma\|_\infty\right\}.$$

For the finite dimensional problem, we want to use the approximating subspace $\Pi_n \equiv \Pi_n^d$. We want to find $\widetilde{u}_n \in \Pi_n$ such that

$$\widetilde{\mathcal{A}}(\widetilde{u}_n,\widetilde{v}) = \widetilde{\ell}_1(\widetilde{v}) + \widetilde{\ell}_2(\widetilde{v}), \qquad \forall \widetilde{v} \in \Pi_n. \tag{17}$$

The Lax-Milgram Theorem (cf. [4, §8.3], [5, §2.7]) implies the existence of u_n for all n. For the error in this Galerkin method, Cea's Lemma (cf. [4, p. 365], [5, p. 62]) implies the convergence of u_n to u, and moreover,

$$\|\widetilde{u} - \widetilde{u}_n\|_1 \leq \frac{\widetilde{c}_{\mathcal{A}}}{\widetilde{c}_e} \inf_{\widetilde{v}\in\Pi_n} \|\widetilde{u} - \widetilde{v}\|_1. \tag{18}$$

It remains to bound the best approximation error on the right side of this inequality.

Ragozin [14] gives bounds on the rate of convergence of best polynomial approximation over the unit ball, and these results are extended in [6] to simultaneous approximation of a function and some of its lower order derivatives. Assume $\widetilde{u} \in C^{m+1}\left(\overline{B}_d\right)$. Using [6, Theorem 1], we have

$$\inf_{\widetilde{v}\in\Pi_n} \|\widetilde{u} - \widetilde{v}\|_1 \leq \frac{c(u,m)}{n^m} \omega_{u,m+1}\left(\frac{1}{n}\right) \tag{19}$$

with

$$\omega_{u,m+1}(\delta) = \sup_{|\alpha|=m+1} \left(\sup_{|x-y|\leq\delta} |D^\alpha \widetilde{u}(x) - D^\alpha \widetilde{u}(y)|\right).$$

The notation $D^\alpha \widetilde{u}(x)$ is standard derivative notation with α a multi-integer. In particular, for $\alpha = (\alpha_1, \ldots, \alpha_d)$,

$$D^\alpha \widetilde{u}(x) = \frac{\partial^{|\alpha|} \widetilde{u}(x_1,\ldots,x_d)}{\partial x_1^{\alpha_1} \cdots \partial x_d^{\alpha_d}}.$$

When (19) is combined with (18), we see that our solutions $\widetilde{u}_n$ converge faster than any power of $1/n$ provided $\widetilde{u} \in C^\infty\left(\overline{B}_d\right)$.

3 A spectral method for $-\Delta u = f$

Consider the Neumann problem for Poisson's equation:

$$-\Delta u = f(s), \qquad s \in \Omega \tag{20}$$

$$\frac{\partial u(s)}{\partial n_s} = g(s), \qquad s \in \partial\Omega \tag{21}$$

As a reference for this problem, see [5, §5.2].

As earlier in (4), we have for functions $u \in H^2(\Omega)$, $v \in H^1(\Omega)$,

$$\int_\Omega v(s)\Delta u(s)\,ds = -\int_\Omega \nabla u(s)\cdot\nabla v(s)\,ds + \int_{\partial\Omega} v(s)\,\frac{\partial u(s)}{\partial n_s}\,ds \tag{22}$$

If this Neumann problem (20)-(21) is solvable, then its solution is not unique: any constant added to a solution gives another solution. In addition, if (20)-(21) is solvable, then

$$\int_\Omega v(s)f(s)\,ds = \int_\Omega \nabla u(s)\cdot\nabla v(s)\,ds - \int_{\partial\Omega} v(s)\,g(s)\,ds \tag{23}$$

Choosing $v(s)\equiv 1$, we obtain

$$\int_\Omega f(s)\,ds = -\int_{\partial\Omega} g(s)\,ds \tag{24}$$

This is a necessary and sufficient condition on the functions f and g in order that (20)-(21) be solvable. With this constraint, the Neumann problem is solvable. To deal with the non-unique solvability, we look for a solution u satisfying

$$\int_\Omega u(s)\,ds = 0 \tag{25}$$

Introduce the bilinear functional

$$\mathcal{A}(v_1,v_2) = \int_\Omega \nabla v_1(s)\cdot\nabla v_2(s)\,ds \tag{26}$$

and the function space

$$\mathcal{V} = \left\{ v\in H^1(\Omega) : \int_\Omega v(s)\,ds = 0 \right\} \tag{27}$$

$\mathcal{A}$ is bounded,

$$|\mathcal{A}(v,w)| \le \|v\|_1\,\|w\|_1, \qquad \forall v,w\in\mathcal{V}.$$

From [5, Prop. 5.3.2] $\mathcal{A}(\cdot,\cdot)$ is strongly elliptic on $\mathcal{V}$, satisfying

$$\mathcal{A}(v,v) \ge c_e\|v\|_1^2, \qquad v\in\mathcal{V}$$

for some $c_e > 0$. The variational form of the Neumann problem (20)-(21) is as follows: find u such that

$$\mathcal{A}(u,v) = \ell_1(v) + \ell_2(v), \qquad \forall v\in\mathcal{V} \tag{28}$$

with ℓ_1 and ℓ_2 defined as in (7)-(8). As before, the Lax-Milgram Theorem implies the existence of a unique solution u to (28) with

$$\|u\|_1 \le \frac{1}{c_e}\left[\|\ell_1\| + \|\ell_2\|\right].$$

As in the preceding section, we transform the problem from being defined over Ω to being over B_d. Most of the arguments are repeated, and we have

$$\widetilde{\mathcal{A}}\left(\widetilde{v}_1, \widetilde{v}_2\right) = \int_{B_d} \left\{\nabla_x \widetilde{v}_1\left(x\right)^{\mathrm{T}} A(x) \nabla_x \widetilde{v}_2\left(x\right)\right\} \left|\det\left[J(x)\right]\right| \, dx.$$

The condition (25) becomes

$$\int_B \widetilde{v}(x) \left|\det\left[J(x)\right]\right| \, dx = 0.$$

We introduce the space

$$\widetilde{\mathcal{V}} = \left\{\widetilde{v} \in H^1\left(B\right) : \int_B \widetilde{v}(x) \left|\det\left[J(x)\right]\right| \, dx = 0\right\}. \tag{29}$$

The Neumann problem now has the reformulation

$$\widetilde{\mathcal{A}}\left(\widetilde{u}, \widetilde{v}\right) = \widetilde{\ell}_1(\widetilde{v}) + \widetilde{\ell}_2\left(\widetilde{v}\right), \qquad \forall \widetilde{v} \in \widetilde{\mathcal{V}} \tag{30}$$

For the finite dimensional approximating problem, we use

$$\widetilde{\mathcal{V}}_n = \widetilde{\mathcal{V}} \cap \Pi_n \tag{31}$$

Then we want to find $\widetilde{u}_n \in \widetilde{\mathcal{V}}_n$ such that

$$\widetilde{a}\left(\widetilde{u}_n, \widetilde{v}\right) = \widetilde{\ell}_1(\widetilde{v}) + \widetilde{\ell}_2\left(\widetilde{v}\right), \qquad \forall \widetilde{v} \in \widetilde{\mathcal{V}}_n \tag{32}$$

We can invoke the standard results of the Lax-Milgram Theorem and Cea's Lemma to obtain the existence of a unique solution $\widetilde{u}_n$, and moreover,

$$\|\widetilde{u} - \widetilde{u}_n\|_1 \leq c \inf_{v \in \widetilde{\mathcal{V}}_n} \|\widetilde{u} - v\|_1. \tag{33}$$

for some $c > 0$. A modification of the argument that led to (19) can be used to obtained a similar result for (33). First, however, we discuss the practical problem of choosing a basis for $\widetilde{\mathcal{V}}_n$.

3.1 Constructing a basis for $\widetilde{\mathcal{V}}_n$

Let $\left\{\varphi_j : 1 \leq j \leq N_n^d\right\}$ denote a basis for Π_n (usually we choose $\left\{\varphi_j\right\}$ to be an orthogonal family in the norm of $L^2\left(B_d\right)$). We assume that $\varphi_1(x)$ is a nonzero constant function. Introduce the new basis elements

$$\widehat{\varphi}_j = \varphi_j - \frac{1}{C} \int_B \varphi_j(x) \left|\det\left[J(x)\right]\right| \, dx, \qquad 1 \leq j \leq N_n^d \tag{34}$$

with

$$C = \int_B \left|\det\left[J(x)\right]\right| \, dx \equiv \left\|\det\left[J\right]\right\|_{L^1} \tag{35}$$

Then $\widehat{\varphi}_1 = 0$ and

$$\begin{aligned}\int_B \widehat{\varphi}_j(x)\,|\det[J(x)]|\,dx &= \int_B \varphi_j(x)\,|\det[J(x)]|\,dx \\ &\quad - \frac{1}{C}\left[\int_B \varphi_j(x)\,|\det[J(x)]|\,dx\right]\left[\int_B |\det[J(x)]|\,dx\right] \\ &= 0\end{aligned}$$

Thus $\left\{\widehat{\varphi}_j : 2 \le j \le N_n^d\right\}$ is a basis of $\widetilde{\mathcal{V}}_n$ and we can use it for our Galerkin procedure in (32).

3.2 The rate of convergence of $\widetilde{u}_n$

Now we estimate $\inf_{v\in\widetilde{\mathcal{V}}_n} \|\widetilde{u} - v\|_1$; see (33). Recalling (34), we consider the linear mapping $P : L^2(B_d) \to L^2(B_d)$ given by

$$\begin{aligned}(P\widetilde{u})(x) &= \widetilde{u}(x) - \frac{1}{C}\int_B |\det[J(y)]|\,\widetilde{u}(y)\,dy, \\ C &= \|\det[J]\|_{L^1};\end{aligned}$$

see (35). The mapping P is a projection

$$\begin{aligned}P(P\widetilde{u})(x) &= (P\widetilde{u})(x) - \frac{1}{C}\int_B |\det[J(y)]|\,(P\widetilde{u})(y)\,dy \\ &= \widetilde{u}(x) - \frac{1}{C}\int_B |\det[J(y)]|\;\widetilde{u}(y)\,dy - \\ &\left(\frac{1}{C}\int_B |\det[J(y)]|\left(\widetilde{u}(y) - \frac{1}{C}\int_B |\det[J(z)]|\;\widetilde{u}(z)\right)\,dy\right) \\ &= \widetilde{u}(x) - \frac{1}{C}\int_B |\det[J(y)]|\;\widetilde{u}(y)\,dy - \frac{1}{C}\int_B |\det[J(y)]|\,\widetilde{u}(y)\,dy \\ &+ \frac{1}{C^2}\underbrace{\int_B |\det[J(y)]|\;dy}_{=C}\int_B |\det[J(z)]|\;\widetilde{u}(z)\,dz \\ &= \widetilde{u}(x) - \frac{1}{C}\int_B |\det[J(y)]|\;\widetilde{u}(y)\,dy \\ &= (P\widetilde{u})(x)\end{aligned}$$

So $P^2 = P$ and P is a projection with $\|P\|_{L^2 \to L^2} \geq 1$ and

$$\begin{aligned}
\|P\widetilde{u}\|_2 &= \|\widetilde{u} - \frac{1}{C}\int_B |\det[J(y)]|\ \widetilde{u}(y)\ dy\|_{L^2} \\
&\leq \|\widetilde{u}\|_{L^2} + \frac{1}{C}\left|\int_B |\det[J(y)]|\ \widetilde{u}(y)\, dy\right| \|1\|_{L^2} \\
&\leq \|\widetilde{u}\|_{L^2} + \frac{1}{C}\|\det[J]\|_{L^2}\|\widetilde{u}\|_{L^2}\sqrt{\frac{\pi^{d/2}}{\Gamma\left(1+\frac{1}{2}d\right)}} \qquad \text{(Cauchy-Schwarz)} \\
&= \left(1 + \sqrt{\frac{\pi^{d/2}}{\Gamma\left(1+\frac{1}{2}d\right)}}\frac{\|\det[J]\|_{L^2}}{\|\det[J]\|_{L^1}}\right)\|\widetilde{u}\|_{L^2} \\
&= c_P\|\widetilde{u}\|_{L^2}
\end{aligned}$$

which shows $\|P\|_{L^2 \to L^2} \leq c_P$ and $\widetilde{\mathcal{V}} := P(H^1(B_d))$, see (29). For $\widetilde{u} \in H^1(B_d)$ we also have $P\widetilde{u} \in H^1(B_d)$ and here we again estimate the norm of P:

$$\begin{aligned}
\|P\widetilde{u}\|_{H^1}^2 &= \|P\widetilde{u}\|_2^2 + \|\nabla(P\widetilde{u})\|_2^2 \\
&\leq c_P^2\|\widetilde{u}\|_2^2 + \|\nabla\widetilde{u}\|_2^2
\end{aligned}$$

since $\nabla(P\widetilde{u}) = \nabla\widetilde{u}$. Furthermore $c_P \geq 1$, so

$$\begin{aligned}
\|P\widetilde{u}\|_{H^1}^2 &\leq c_P^2\|\widetilde{u}\|_{L^2}^2 + c_P^2\|\nabla\widetilde{u}\|_{L^2}^2 \\
&= c_P^2(\|\widetilde{u}\|_{L^2}^2 + \|\nabla\widetilde{u}\|_{L^2}^2) \\
&= c_P^2\|\widetilde{u}\|_{H^1}^2 \\
\|P\widetilde{u}\|_{H^1} &\leq c_P\|\widetilde{u}\|_{H^1}
\end{aligned}$$

and we have also $\|P\|_{H^1 \to H^1} \leq c_P$. For $\widetilde{u} \in \widetilde{\mathcal{V}} = P(H^1(B))$ we can now estimate the minimal approximation error

$$\begin{aligned}
\min_{\widetilde{p}\in\widetilde{\mathcal{V}}_n}\|\widetilde{u} - \widetilde{p}\|_{H_1} \quad &= \quad \min_{\widetilde{p}\in\widetilde{\mathcal{V}}_n}\|P\widetilde{u} - \widetilde{p}\|_{H_1} && P \text{ is a projection and } \widetilde{u} \in \text{image}(P) \\
&= \quad \min_{p\in\Pi_n}\|P\widetilde{u} - Pp\|_{H_1} && \text{because } \widetilde{\mathcal{V}}_n = P(\Pi_n) \\
&\leq \quad \min_{p\in\Pi_n}\|P\|_{H^1\to H^1}\|\widetilde{u} - p\|_{H_1} \\
&\leq \quad c_P \min_{p\in\Pi_n}\|\widetilde{u} - p\|_{H_1}
\end{aligned}$$

and now we can apply the results from [6].

4 Implementation

Consider the implementation of the Galerkin method of §2 for the Neumann problem (1)-(2) over Ω by means of the reformulation in (15) over the unit ball B_d. We are to find the function $\widetilde{u}_n \in \Pi_n$ satisfying (15). To do so, we begin by

selecting a basis for Π_n, denoting it by $\{\varphi_1, \ldots, \varphi_N\}$, with $N \equiv N_n = \dim \Pi_n$. Generally we use a basis that is orthonormal in the norm of $L^2(B_2)$. It would be better probably to use a basis that is orthonormal in the norm of $H^1(B_d)$; for example, see [18]. We seek

$$\widetilde{u}_n(x) = \sum_{k=1}^{N} \alpha_k \varphi_k(x) \tag{36}$$

Then (17) is equivalent to

$$\begin{aligned} \sum_{k=1}^{N} \alpha_k \int_{B_d} \left[\sum_{i,j=1}^{d} a_{i,j}(x) \frac{\partial \varphi_k(x)}{\partial x_j} \frac{\partial \varphi_\ell(x)}{\partial x_i} + \gamma(x) \varphi_k(x) \varphi_\ell(x) \right] |\det [J(x)]| \, dx \\ = \int_{B_d} f(x) \, \varphi_\ell(x) \, |\det [J(x)]| \, dx \\ + \int_{\partial B_d} g(x) \, \varphi_\ell(x) \, |J_{bdy}(x)| \, dx, \qquad \ell = 1, \ldots, N \end{aligned} \tag{37}$$

The function $|J_{bdy}(x)|$ arises from the transformation of an integral over $\partial\Omega$ to one over ∂B_d, associated with the change from ℓ_2 to $\widetilde{\ell}_2$ as discussed preceding (15). For example, in one variable the boundary $\partial\Omega$ is often represented as a mapping

$$\chi(\theta) = (\chi_1(\theta), \chi_2(\theta)), \qquad 0 \le \theta \le 2\pi.$$

In that case, $|J_{bdy}(x)|$ is simply $|\chi'(\theta)|$ and the associated integral is

$$\int_0^{2\pi} g(\chi(\theta)) \, \varphi_\ell(\chi(\theta)) \, |\chi'(\theta)| \, d\theta$$

In (37) we need to calculate the orthonormal polynomials and their first partial derivatives; and we also need to approximate the integrals in the linear system. For an introduction to the topic of multivariate orthogonal polynomials, see Dunkl and Xu [10] and Xu [17]. For multivariate quadrature over the unit ball in $\mathbb{R}^d$, see Stroud [16].

For the Neumann problem (20)-(21) of §3, the implementation is basically the same. The basis $\{\varphi_1, \ldots, \varphi_N\}$ is modified as in (34), with the constant C of (35) approximated using the quadrature in (42), given below.

4.1 The planar case

The dimension of Π_n is

$$N_n = \frac{1}{2}(n+1)(n+2) \tag{38}$$

For notation, we replace x with (x, y). How do we choose the orthonormal basis $\{\varphi_\ell(x, y)\}_{\ell=1}^{N}$ for Π_n? Unlike the situation for the single variable case, there are many possible orthonormal bases over $B_d = D$, the unit disk in $\mathbb{R}^2$. We have

chosen one that is particularly convenient for our computations. These are the "ridge polynomials" introduced by Logan and Shepp [12] for solving an image reconstruction problem. We summarize here the results needed for our work.

Let

$$\mathcal{V}_n = \{P \in \Pi_n : (P, Q) = 0 \quad \forall Q \in \Pi_{n-1}\}$$

the polynomials of degree n that are orthogonal to all elements of Π_{n-1}. Then the dimension of $\mathcal{V}_n$ is $n+1$; moreover,

$$\Pi_n = \mathcal{V}_0 \oplus \mathcal{V}_1 \oplus \cdots \oplus \mathcal{V}_n \tag{39}$$

It is standard to construct orthonormal bases of each $\mathcal{V}_n$ and to then combine them to form an orthonormal basis of Π_n using the latter decomposition. As an orthonormal basis of $\mathcal{V}_n$ we use

$$\varphi_{n,k}(x,y) = \frac{1}{\sqrt{\pi}} U_n\left(x\cos(kh) + y\sin(kh)\right), \quad (x,y) \in D, \quad h = \frac{\pi}{n+1} \tag{40}$$

for $k = 0, 1, \ldots, n$. The function U_n is the Chebyshev polynomial of the second kind of degree n:

$$U_n(t) = \frac{\sin(n+1)\,\theta}{\sin\theta}, \qquad t = \cos\theta, \quad -1 \le t \le 1, \quad n = 0, 1, \ldots \tag{41}$$

The family $\left\{\varphi_{n,k}\right\}_{k=0}^{n}$ is an orthonormal basis of $\mathcal{V}_n$. As a basis of Π_n, we order $\left\{\varphi_{n,k}\right\}$ lexicographically based on the ordering in (40) and (39):

$$\{\varphi_\ell\}_{\ell=1}^{N} = \left\{\varphi_{0,0},\, \varphi_{1,0},\, \varphi_{1,1},\, \varphi_{2,0},\, \ldots,\, \varphi_{n,0},\, \ldots, \varphi_{n,n}\right\}$$

To calculate the first order partial derivatives of $\varphi_{n,k}(x,y)$, we need $U_n^{'}(t)$. The values of $U_n(t)$ and $U_n^{'}(t)$ are evaluated using the standard triple recursion relations

$$\begin{aligned} U_{n+1}(t) &= 2tU_n(t) - U_{n-1}(t) \\ U_{n+1}^{'}(t) &= 2U_n(t) + 2tU_n^{'}(t) - U_{n-1}^{'}(t) \end{aligned}$$

For the numerical approximation of the integrals in (37), which are over B being the unit disk, we use the formula

$$\int_B g(x,y)\,dx\,dy \approx \sum_{l=0}^{q} \sum_{m=0}^{2q} g\left(r_l, \frac{2\pi\, m}{2q+1}\right) \omega_l \frac{2\pi}{2q+1} r_l \tag{42}$$

Here the numbers ω_l are the weights of the $(q+1)$-point Gauss-Legendre quadrature formula on $[0,1]$. Note that

$$\int_0^1 p(x)dx = \sum_{l=0}^{q} p(r_l)\omega_l,$$

for all single-variable polynomials $p(x)$ with $\deg(p) \le 2q+1$. The formula (42) uses the trapezoidal rule with $2q+1$ subdivisions for the integration over $\overline{B}_d$ in the azimuthal variable. This quadrature is exact for all polynomials $g \in \Pi_{2q}$. This formula is also the basis of the hyperinterpolation formula discussed in [11].

4.2 The three dimensional case

In the three dimensional case the dimension of Π_n is given by

$$N_n = \binom{n+3}{3}$$

and we choose the following orthogonal polynomials on the unit ball

$$\begin{aligned}\varphi_{m,j,\beta}(x) &= c_{m,j} p_j^{(0,m-2j+\frac{1}{2})}(2\|x\|^2-1) S_{\beta,m-2j}(x) \\ &= c_{m,j}\|x\|^{m-2j} p_j^{(0,m-2j+\frac{1}{2})}(2\|x\|^2-1) S_{\beta,m-2j}\left(\frac{x}{\|x\|}\right), \qquad (43)\\ j &= 0,\ldots,\lfloor m/2\rfloor, \quad \beta = 0,1,\ldots,2(m-2j), \quad m = 0,1,\ldots,n\end{aligned}$$

The constants $c_{m,j}$ are given by $c_{m,j} = 2^{\frac{5}{4}+\frac{m}{2}-j}$; and the functions $p_j^{(0,m-2j+\frac{1}{2})}$ are the normalized Jacobi polynomials. The functions $S_{\beta,m-2j}$ are spherical harmonic functions and they are orthonormal on the sphere $\mathbb{S}^2 \subset \mathbb{R}^3$. See [10, 3] for the definition of these functions. In [3] one also finds the quadrature methods which we use to approximate the integrals over $B_1(0)$ in (14) and (15). The functional $\widetilde{\ell}_2$ in (15) is given by

$$\begin{aligned}\widetilde{\ell}_2(v) \quad = \quad & \int_0^{\pi}\int_0^{2\pi} g(\Phi(\Upsilon(1,\theta,\phi))) \qquad (44)\\ & \cdot\|(\Phi\circ\Upsilon)_\theta(1,\theta,\phi)\times(\Phi\circ\Upsilon)_\phi(1,\theta,\phi)\|\, v(\Phi(\Upsilon(1,\theta,\phi)))d\phi\, d\theta\end{aligned}$$

where

$$\Upsilon(\rho,\theta,\phi) := \rho\,(\sin(\theta)\cos(\phi), \sin(\theta)\sin(\phi), \cos(\theta)) \qquad (45)$$

is the usual transformation between spherical and Cartesian coordinates and the indices denote the partial derivatives. For the numerical approximation of the integral in (44) we use traezoidal rules in the ϕ direction and Gauß-Legendre formulas for the θ direction.

5 Numerical examples

The construction of our examples is very similar to that given in [3] for the Dirichlet problem. Our first two transformations Φ have been so chosen that we can invert explicitly the mapping Φ, to be able to better construct our test examples. **This is not needed when applying the method**; but it simplifies the construction of our test cases. Given Φ, we need to calculate analytically the matrix

$$A(x) = J(x)^{-1} J(x)^{-\mathrm{T}}. \qquad (46)$$

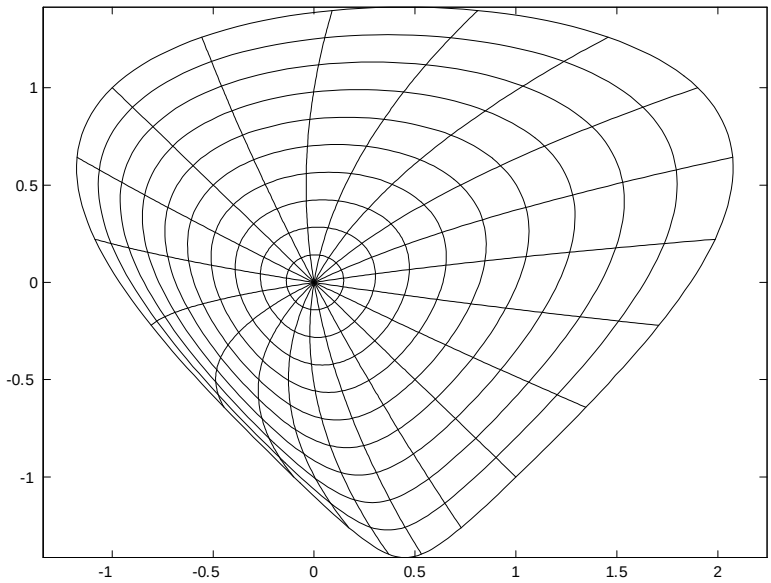

Figure 1: Images of (47), with $a = 0.5$, for lines of constant radius and constant azimuth on the unit disk.

5.1 The planar case

For our variables, we replace a point $x \in B_d$ with (x, y), and we replace a point $s \in \Omega$ with (s, t). Define the mapping $\Phi : \overline{B} \to \overline{\Omega}$ by $(s, t) = \Phi(x, y)$,

$$\begin{aligned} s &= x - y + ax^2 \\ t &= x + y \end{aligned} \tag{47}$$

with $0 < a < 1$. It can be shown that Φ is a 1-1 mapping from the unit disk $\overline{B}$. In particular, the inverse mapping $\Psi : \overline{\Omega} \to \overline{B}$ is given by

$$\begin{aligned} x &= \frac{1}{a}\left[-1 + \sqrt{1 + a(s+t)}\right] \\ y &= \frac{1}{a}\left[at - \left(-1 + \sqrt{1 + a(s+t)}\right)\right] \end{aligned} \tag{48}$$

In Figure 1, we give the images in $\overline{\Omega}$ of the circles $r = j/10$, $j = 1, \ldots, 10$ and the azimuthal lines $\theta = j\pi/10$, $j = 1, \ldots, 20$.

The following information is needed when implementing the transformation from $-\Delta u + \gamma u = f$ on Ω to a new equation on B:

$$D\Phi = J(x, y) = \begin{pmatrix} 1 + 2ax & -1 \\ 1 & 1 \end{pmatrix}$$

$$\det(J) = 2(1 + ax)$$

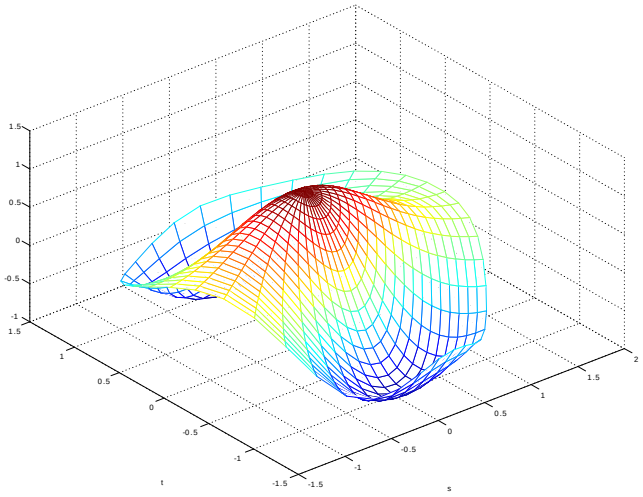

Figure 2: The function $u(s,t)$ of (50)

$$J(x)^{-1} = \frac{1}{2(1+ax)} \begin{pmatrix} 1 & 1 \\ -1 & 1+2ax \end{pmatrix}$$

$$A = J(x)^{-1} J(x)^{-\mathrm{T}} = \frac{1}{2(1+ax)^2} \begin{pmatrix} 1 & ax \\ ax & 2a^2x^2 + 2ax + 1 \end{pmatrix}$$

The latter are the coefficients needed to define $\widetilde{\mathcal{A}}$ in (14).

We give numerical results for solving the equation

$$-\Delta u(s,t) + e^{s-t} u(s,t) = f(s,t), \qquad (s,t) \in \Omega \tag{49}$$

As a test case, we choose

$$u(s,t) = e^{-s^2} \cos(\pi t), \qquad (s,t) \in \Omega \tag{50}$$

The solution is pictured in Figure 2. To find $f(s,t)$, we use (49) and (50). We use the domain parameter $a = 0.5$, with Ω pictured in Figure 1.

Numerical results are given in Table 1 for even values of n. The integrations in (37) were performed with (42); and the integration parameter q ranged from 10 to 30. We give the condition numbers of the linear system (37) as produced in MATLAB. To calculate the error, we evaluate the numerical solution and the error on the grid

$$\Phi(x_{i,j}, y_{i,j}) = \Phi(r_i \cos\theta_j, r_i \sin\theta_j)$$

$$(r_i, \theta_j) = \left(\frac{i}{10}, \frac{j\pi}{10}\right), \qquad i = 0, 1, \ldots 10; \quad j = 1, \ldots 20$$

Table 1: Maximum errors in Galerkin solution u_n

n	N_n	$\|u-u_n\|_\infty$	$cond$	n	N_n	$\|u-u_n\|_\infty$	$cond$
2	6	$9.71E-1$	14.5	14	120	$3.90E-5$	6227
4	15	$2.87E-1$	86.1	16	153	$6.37E-6$	10250
6	28	$5.85E-2$	309	18	190	$8.20E-7$	15960
8	45	$1.16E-2$	824	20	231	$9.44E-8$	23770
10	66	$2.26E-3$	1819	22	276	$1.06E-8$	34170
12	91	$2.81E-4$	3527	24	325	$1.24E-9$	47650

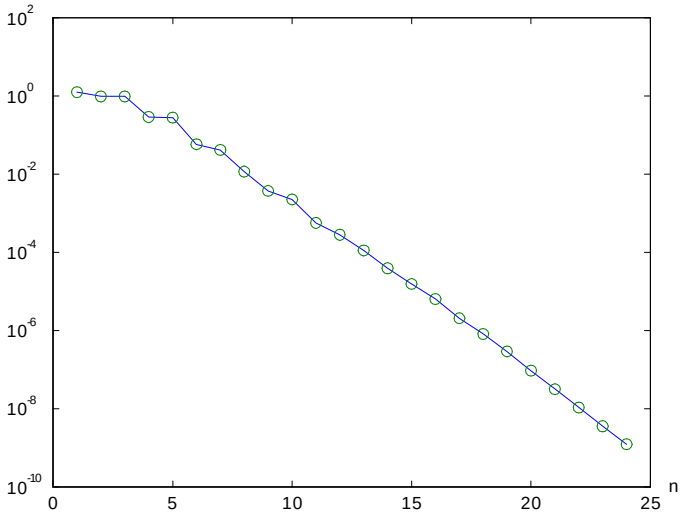

Figure 3: Errors from Table 1

The results are shown graphically in Figure 3. The use of a semi-log scale demonstrates the exponential convergence of the method as the degree increases.

To examine experimentally the behaviour of the condition numbers for the linear system (37), we have graphed the condition numbers from Table 1 in Figure 4. Note that we are graphing N_n^2 vs. the condition number of the associated linear system. The graph seems to indicate that the condition number of the system (37) is directly proportional to the square of the order of the system, with the order given in (38).

For the Poisson equation

$$-\Delta u\,(s,t) = f\,(s,t)\,, \qquad (s,t) \in \Omega$$

with the same true solution as in (50), we use the numerical method given in §3. The numerical results are comparable. For example, with $n = 20$, we obtain

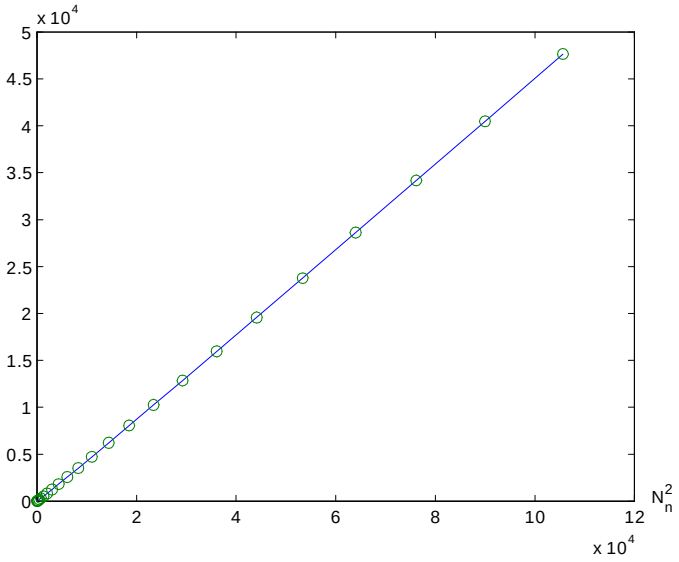

Figure 4: Condition numbers from Table 1

$\|u - u_n\|_\infty = 9.90 \times 10^{-8}$ and the condition number is approximately 14980.

5.2 The three dimensional case

To illustrate that the proposed spectral method converges rapidly, we first use a simple test example. We choose the linear transformation

$$s := \Phi_1(x) = \begin{pmatrix} x_1 - 3x_2 \\ 2x_1 + x_2 \\ x_1 + x_2 + x_3 \end{pmatrix},$$

so that $B_1(0)$ is transformed to an ellipsoid Ω_1; see figure 5. For this transformation $D\Phi_1$ and $J_1 = \det(D\Phi_1)$ are constant functions. For a test solution, we use the function

$$u(s) = s_1 e^{s_2} \sin(s_3) \tag{51}$$

which is analytic in each variable.

Table 2 shows the errors and the development of the condition numbers for the solution of (1) on Ω_1. The associated graphs for the errors and condition numbers are shown in figures 6 and 7, respectively. The graph of the error is consistent with exponential convergence; and the condition number seems to have a growth proportional to the square of the number of degrees of freedom N_n.

Next we study domains Ω which are star shaped with respect to the origin,

$$\Omega_2 = \{x \in \mathbb{R}^3 \mid x = \Upsilon(\rho, \theta, \phi), \quad 0 \le \rho \le R(\theta, \phi)\}. \tag{52}$$

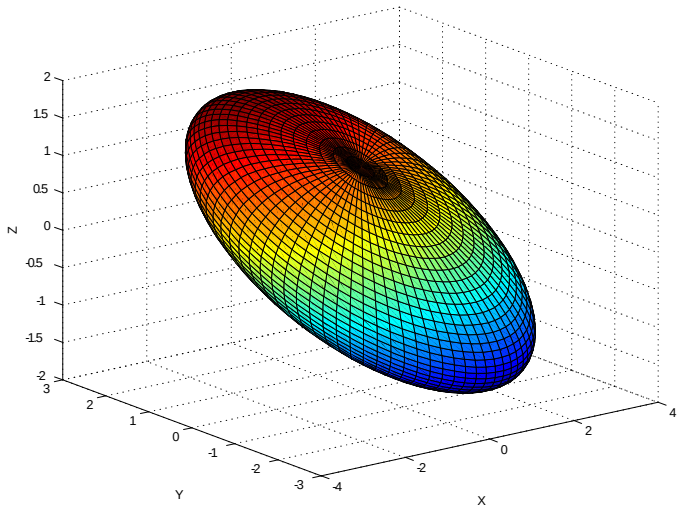

Figure 5: The boundary of Ω_1

See (45) for the definition of Υ, and $R : \mathbb{S}^2 \to (0, \infty)$ is assumed to be a C^∞ function. In this case we can construct arbitrarily smooth and invertible mappings $\Phi : B_1(0) \to \Omega_2$ as we will show now. First we define a function $t : [0, 1] \to [0, 1]$

$$t(\rho) := \begin{cases} 0, & 0 \le \rho \le \frac{1}{2}, \\ 2^{e_s}(\rho - \frac{1}{2})^{e_s}, & \frac{1}{2} < \rho \le 1. \end{cases} \tag{53}$$

the parameter $e_s \in \mathbb{N}$ determines the smoothness of $t \in C^{e_s - 1}[0, 1]$. For the following we will assume that $R(\theta, \phi) > 1$, for all θ and ϕ; this follows after an appropriate scaling of the problem. With the help of t we define the function $\tilde{R}$ which is monotone increasing from 0 to $R(\theta, \phi)$ on $[0, 1]$ and equal to the

Table 2: Maximum errors in Galerkin solution u_n

n	N_n	$\|u - u_n\|_\infty$	$cond$	n	N_n	$\|u - u_n\|_\infty$	$cond$
1	4	$9.22E+00$	8	9	220	$4.15E-04$	1964
2	10	$5.25E+00$	31	10	286	$6.84E-05$	2794
3	20	$1.92E+00$	79	11	364	$1.11E-05$	3862
4	35	$5.80E-01$	167	12	455	$1.60E-06$	5211
5	56	$1.62E-01$	314	13	560	$2.06E-07$	6888
6	84	$4.53E-02$	540	14	680	$2.60E-08$	8937
7	120	$1.03E-02$	871	15	816	$3.01E-09$	11415
8	165	$2.31E-03$	1335	16	969	$3.13E-10$	14376

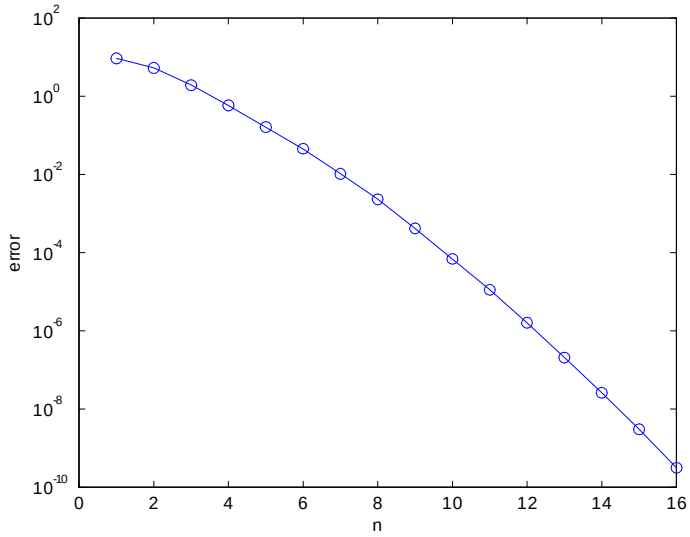

Figure 6: Errors from Table 2

identity on $[0, 1/2]$,

$$\widetilde{R}(\rho, \theta, \phi) := t(\rho)R(\theta, \phi) + (1 - t(\rho))\rho$$

Because

$$\frac{\partial}{\partial \rho}\widetilde{R}(\rho, \theta, \phi) = t'(\rho)(R(\theta, \phi) - \rho) + (1 - t(\rho)) > 0, \quad \rho \in [0, 1]$$

the function $\widetilde{R}$ is an invertible function of ρ of class C^{e_s-1}. The transformation $\Phi_2 : B_1(0) \to \Omega_2$ is defined by

$$\Phi_2(x) := \Upsilon(\widetilde{R}(\rho, \theta, \phi), \theta, \phi), \quad x = \Upsilon(\rho, \theta, \phi) \in B_1(0)$$

The properties of $\widetilde{R}$ imply that Φ_2 is equal to the identity on $B_{\frac{1}{2}}(0)$ and the outside shell $B_1(0) \setminus B_{\frac{1}{2}}(0)$ is deformed by Φ_2 to cover $\Omega_2 \setminus B_{\frac{1}{2}}(0)$.

For a test surface, we use

$$\begin{aligned} R(\theta, \phi) &= 2 + \frac{3}{4}\cos(2\phi)\sin(\theta)^2(7\cos(\theta)^2 - 1) \\ e_s &= 5; \end{aligned} \tag{54}$$

see figures 8-9 for pictures of $\partial\Omega_2$. For our test example, we use u from (51).

The term $\cos(2\phi)\sin(\theta)^2(7\cos(\theta)^2-1)$ is a spherical harmonic function which shows $R \in C^\infty(\mathbb{S}^2)$, and the factor $3/4$ is used to guarantee $R > 1$. For the

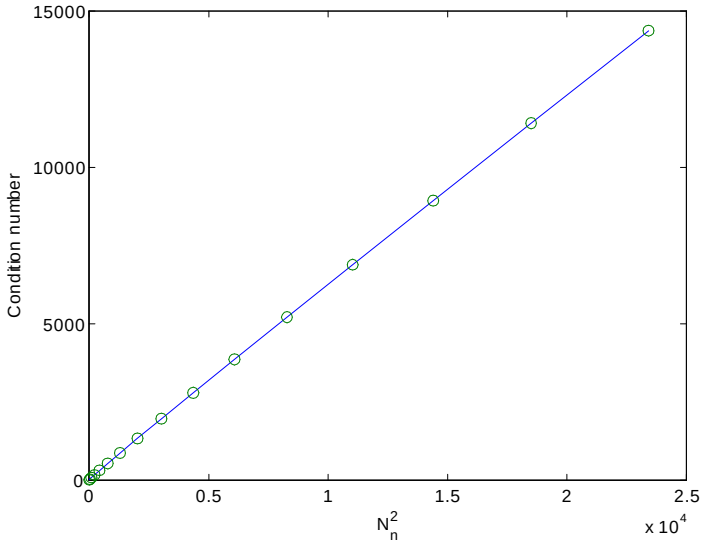

Figure 7: Conditions numbers from Table 2

transformation Φ_2 we get $\Phi_2 \in C^4(B_1(0))$, so we expect a convergence of order $O(n^{-4})$. Our spectral method will now approximate $u \circ \Phi_2$ on the unit ball, which varies much more than the function in our first example.

We also note that one might ask why we do not further increase e_s (see (53)) to get a better order of convergence. It is possible to do this, but the price one pays is in larger derivatives of $u \circ \Phi_2$, and this may result in larger errors for the range of n values where we actually calculate the approximation. The search for an optimal e_s is a problem on its own, but it also depends on the solution u. So we have chosen $e_s = 5$ in order to demonstrate our method, showing that the qualitative behaviour of the error is the same as in our earlier examples.

The results of our calculations are given in table 3, and the associated graphs of the errors and condition numbers are shown in figures 10 and 11, respectively. The graph in Figure 11 shows that the condition numbers of the systems grow more slowly than in our first example, but again the condition numbers appear to be proportional to N_n^2. The graph of the error in Figure 10 again resembles a line and this implies exponential convergence; but the line has a much smaller slope than in the first example so that the error is only reduced to about 0.02 when we use degree 16. What we expect is a convergence of order $O(n^{-4})$, but the graph does not reveal this behavior in the range of n values we have used. Rather, the convergence appears to be exponential. In the future we plan on repeating this numerical example with an improved extension Φ of the boundary given in (54).

When given a mapping $\varphi : \partial B \to \partial\Omega$, it is often nontrivial to find an

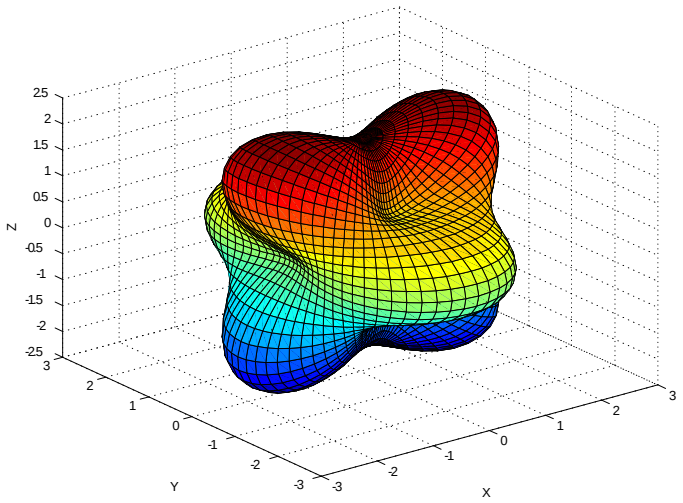

Figure 8: A view of $\partial\Omega_2$

extension $\Phi : \overline{B} \xrightarrow[onto]{1-1} \overline{\Omega}$ with $\Phi|_{\partial B} = \varphi$ and with other needed properties. For example, consider a star-like region Ω whose boundary surface $\partial\Omega$ is given by

$$\rho = R(\theta, \phi)$$

with $R : \mathbb{S}^2 \to \partial\Omega$. It might seem natural to use

$$\Phi(\rho, \theta, \phi) = \rho R(\theta, \phi), \quad 0 \le \rho \le 1, \quad 0 \le \theta \le \pi, \quad 0 \le \phi \le 2\pi$$

However, such a function Φ is not continuously differentiable at $\rho = 0$. We are exploring this general problem, looking at ways of producing Φ with the properties that are needed for implementing our spectral method.

ACKNOWLEDGEMENTS. The authors would like to thank Professor Weimin Han for his careful proofreading of the manuscript.

References

[1] M. Abramowitz, I.A. Stegun, *Handbook of Mathematical Functions*, Dover Publications, Inc., New York, 1965.

[2] K. Atkinson. *An Introduction to Numerical Analysis*, 2nd ed., John Wiley, New York, 1989.

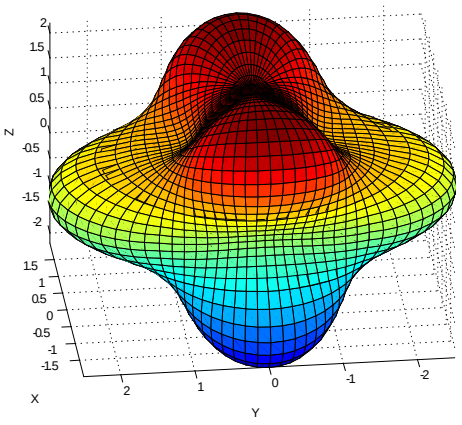

Figure 9: Another view of $\partial\Omega_2$

[3] K. Atkinson, D. Chien, and O. Hansen, A Spectral Method for Elliptic Equations: The Dirichlet Problem, *Advances in Computational Mathematics*, DOI: 10.1007/s10444-009-9125-8, to appear.

[4] K. Atkinson and W. Han. *Theoretical Numerical Analysis: A Functional Analysis Framework*, 2nd ed., Springer-Verlag, New York, 2005.

[5] S. Brenner and L. Scott, *The Mathematical Theory of Finite Element Methods*, Springer-Verlag, 1994.

[6] T. Bagby, L. Bos, and N. Levenberg, Multivariate simultaneous approximation, *Constructive Approximation*, **18** (2002), pp. 569-577.

Table 3: Maximum errors in Galerkin solution u_n

n	N_n	$\|u-u_n\|_\infty$	*cond*	n	N_n	$\|u-u_n\|_\infty$	*cond*
1	4	2.322	3	9	220	0.268	475
2	10	1.321	10	10	286	0.231	701
3	20	1.085	19	11	364	0.151	987
4	35	1.152	44	12	455	0.116	1350
5	56	1.010	73	13	560	0.068	1809
6	84	0.807	125	14	680	0.053	2406
7	120	0.545	203	15	816	0.038	3118
8	165	0.404	318	16	969	0.022	3967

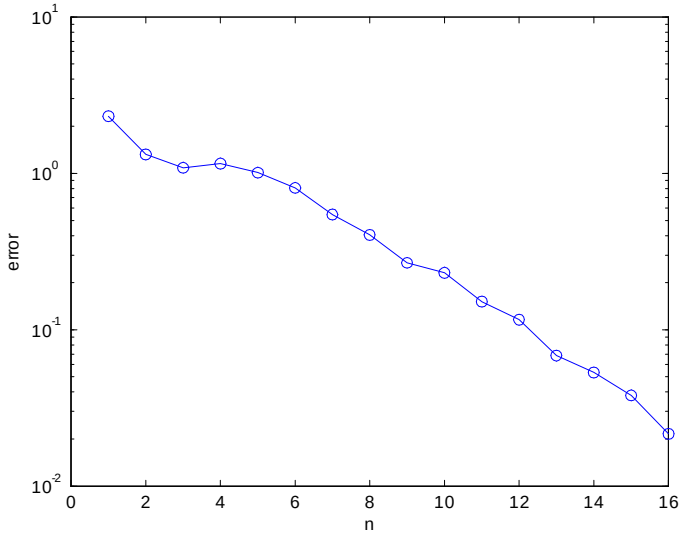

Figure 10: Errors from table 3

[7] C. Canuto, A. Quarteroni, My. Hussaini, and T. Zang, *Spectral Methods in Fluid Mechanics*, Springer-Verlag, 1988.

[8] C. Canuto, A. Quarteroni, My. Hussaini, and T. Zang, *Spectral Methods - Fundamentals in Single Domains*, Springer-Verlag, 2006.

[9] E. Doha and W. Abd-Elhameed. Efficient spectral-Galerkin algorithms for direct solution of second-order equations using ultraspherical polynomials, *SIAM J. Sci. Comput.* **24** (2002), 548-571.

[10] C. Dunkl and Y. Xu. *Orthogonal Polynomials of Several Variables*, Cambridge Univ. Press, Cambridge, 2001.

[11] O. Hansen, K. Atkinson, and D. Chien. On the norm of the hyperinterpolation operator on the unit disk and its use for the solution of the nonlinear Poisson equation, *IMA J. Numerical Analysis*, **29** (2009), pp. 257-283, DOI: 10.1093/imanum/drm052.

[12] B. Logan. and L. Shepp. Optimal reconstruction of a function from its projections, *Duke Mathematical Journal* **42**, (1975), 645–659.

[13] W. McLean, *Strongly Elliptic Systems and Boundary Integral Equations*, Cambridge Univ. Press, 2000.

[14] D. Ragozin. Constructive polynomial approximation on spheres and projective spaces, *Trans. Amer. Math. Soc.* **162** (1971), 157-170.

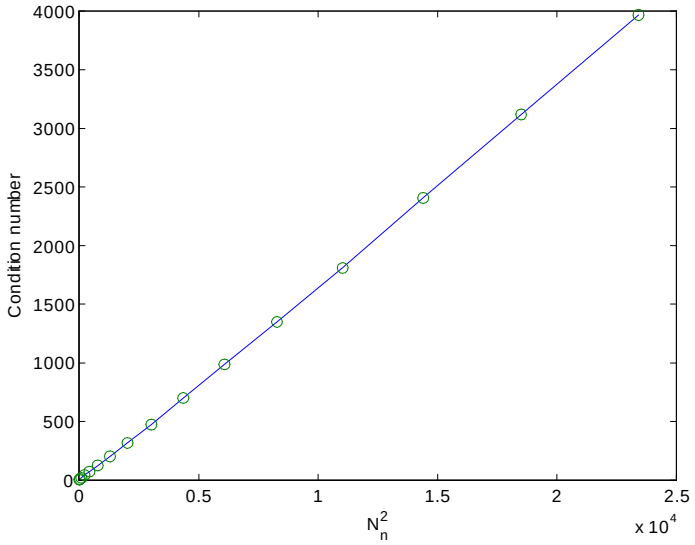

Figure 11: Condition numbers from table 3

[15] J. Shen and L. Wang. Analysis of a spectral-Galerkin approximation to the Helmholtz equation in exterior domains, *SIAM J. Numer. Anal.* **45** (2007), 1954-1978.

[16] A. Stroud. *Approximate Calculation of Multiple Integrals,* Prentice-Hall, Inc., Englewood Cliffs, N.J., 1971.

[17] Yuan Xu. Lecture notes on orthogonal polynomials of several variables, in *Advances in the Theory of Special Functions and Orthogonal Polynomials*, Nova Science Publishers, 2004, 135-188.

[18] Yuan Xu. A family of Sobolev orthogonal polynomials on the unit ball, *J. Approx. Theory* **138** (2006), 232-241.